

The editorial support team
Atmospheric Chemistry and Physics
October 15th, 2023
Subject: Revision of manuscript egusphere-2023-1608

Dear Editors and Reviewers:

Thank you for your letter and for giving us the opportunity to revise our manuscript on “Identification of stratospheric disturbance information in China based on round-trip intelligent sounding system” [Paper # egusphere-2023-1608]. We have carefully reviewed the comments and have revised the manuscript accordingly. Our responses are given in a point-by-point manner below. Changes to the manuscript are shown in the revised manuscript with “track changes”.

Sincerely,

Yang He

E-mail: heyang12357@sina.com

Corresponding author: Zheng Sheng

E-mail: 19994035@sina.com

Response to Reviewer #2:

General comments:

This study applies the structure function and singular measure to quantify the stratospheric small-scale gravity wave (SGW) over China by Hurst parameter and intermittency parameter, and discuss its relationship with inertia-gravity wave (IGW). The introduced observation system for floating balloon measurements is an interesting novel option to investigate atmospheric disturbances in the stratosphere. Although the authors’ dataset and observation could be of very high scientific value, the study in its present form suffers from several flaws and I recommend publication with suitable revisions.

Response: Thanks for appreciating our contribution and performing such an insightful and detailed review. We have made targeted revisions and replied in accordance with the specific opinions you give later. Your professional opinions are very valuable for improving the quality of our manuscript. We also look forward to your feedback on our improved work.

Specific comments:

1) The dynamics of a sounding platform and its response to atmospheric motions is of necessary knowledge before interpreting atmospheric disturbances parameter such as structure functions and intermittency parameter.

In the present case, the expected behavior of the balloon in the flat-floating phase remains unclear. From the introduction (L84-89), it is implied that this phase is characterized by quasi-horizontal motion similar to superpressure balloons (Hertzog et al., 2002; Boccara et al., 2008). Whether their detection principles are consistent? the authors should further explain the uniqueness of the detection system, and strongly recommend that the dynamic

process of detection be further elaborated.

Response: Thanks for your comments, in fact, the balloons we use are zero-pressure balloons, which are not the same as overpressure balloons.

Zero-pressure balloon is made of low-temperature polyethylene film, the ball itself is not closed, gravity and buoyancy are balanced during flat-floating stage, the bottom of the exhaust pipe so that the ball inside and outside the pressure difference is basically zero, the flight time is short (several hours). The overpressure balloon sphere is closed, and the structure of the sphere is similar to that of the pumpkin shape. The volume of the sphere is basically unchanged, and the flight time is longer (several weeks).

the detection principle of RTISS in three stages is given below

In the ascending phase, the balloon is driven without power in the horizontal direction, which can be approximated as moving with the wind field and subjected to buoyancy, gravity and air resistance in the vertical direction(Cao et al., 2019; He et al., 2020):

$$m \frac{dw}{dt} = \rho V g - mg - \frac{\pi}{8} \rho C_p D^2 w^2$$

Where m is the mass of the system, g is the acceleration of gravity, w is the vertical velocity of the balloon, V is the volume of the outer sphere, ρ is the atmospheric density, C_p is the drag coefficient, and D is the diameter of the outer sphere.

In the horizontal floating stage, the adaptive flat-floating process is realized by controlling an appropriate net lift force from the ground. Under this condition, the vertical force is dynamically balanced, and the balloon trajectory can be regarded as an approximate horizontal motion. The motion equations are written as:

$$F_{up} = \rho_0 g \frac{V_h P_h T_0}{T_h P_0} - mg$$

$$V_h = mg / \rho_h$$

Where T_h , P_h , and ρ_h are the temperature, air pressure, and density inside the balloon at height h , T_0 , P_0 , and ρ_0 are the initial temperature, air pressure and density before the balloon is released.

In the descending stage, the radiosonde descends under the parachute, from the low-density atmosphere into the high-density atmosphere, the motion equations at this time are:

$$m \frac{dV_{ux}}{dt} = -m_{au} \frac{dV_x}{dt} - \frac{\rho S V_r (C_d V_x + C_l (k V_y - j V_z))}{2}$$

$$m \frac{dV_{uy}}{dt} = -m_{au} \frac{dV_y}{dt} - \frac{\rho S V_r (C_d V_y + C_l (-k V_x + i V_z))}{2}$$

$$m \frac{dV_{uz}}{dt} = m_f g - mg - m_{au} \frac{dV_z}{dt} - \rho S V_r (C_d V_z + C_l (j V_x - i V_y)) / 2$$

$$V_r = \sqrt{V_x^2 + V_y^2 + V_z^2}$$

Where m is the total mass of the system, m_{au} is the additional mass (produced by the acceleration of the parachute), and m_f is the air mass discharged by the system. V_x , V_y and V_z are the velocity of the system relative to the air, V_{ux} , V_{uy} and V_{uz} are the velocity of the radiosonde itself, C_d and C_l are the drag coefficient and the lift coefficient, and i , j , and k are the cosines of the direction vector.

Considering that the specific physical process regarding the detection process has been

given in a previously published paper, here we make the following modifications:

L89 Added: “The detection system has different working principles in the three stages, and the specific dynamic process can be referred to the previous work (Cao et al., 2019). It should be noted that the RTISS uses the zero-pressure balloon to meet the needs of low-cost business observation, which is different from the superpressure balloon (Hertzog et al., 2002; Boccara et al., 2008). For the zero-pressure balloon, the bottom exhaust pipe makes the pressure difference between inside and outside the balloon basically zero, the flight time is short (several hours). While for the super-pressure balloon, the sphere is closed, the volume of the sphere is basically unchanged, and the flight time is longer (several weeks).”

2) the authors carry out their structure function analysis in space coordinate (longitudinal distance) after interpolation, in my intuition, time is the appropriate and most commonly used coordinate in which to perform the analysis similar to a quasi-Lagrange measurement. Of course, this may be treated differently from the linear fitting mentioned in the first point, I am well aware that different methods have their own rationality and limitations, and it may be interesting if the author can compare the results of different methods here. For example, compare the results in space and time coordinates? If the data can be analyzed in time coordinates, there is no need for interpolation since the measurements were sampled regularly.

Yes, we have also considered the way you mentioned, that is, after linear fitting according to the flat drift trajectory, the fitting direction is taken as the separation distance direction. Let's take the YC case on October 15th in Figure 3 as an example to illustrate this method. First, the trajectory of flat-floating stage, and the variation of X coordinate, Y coordinate, and Z coordinate during flat-floating stage are plotted as follows:

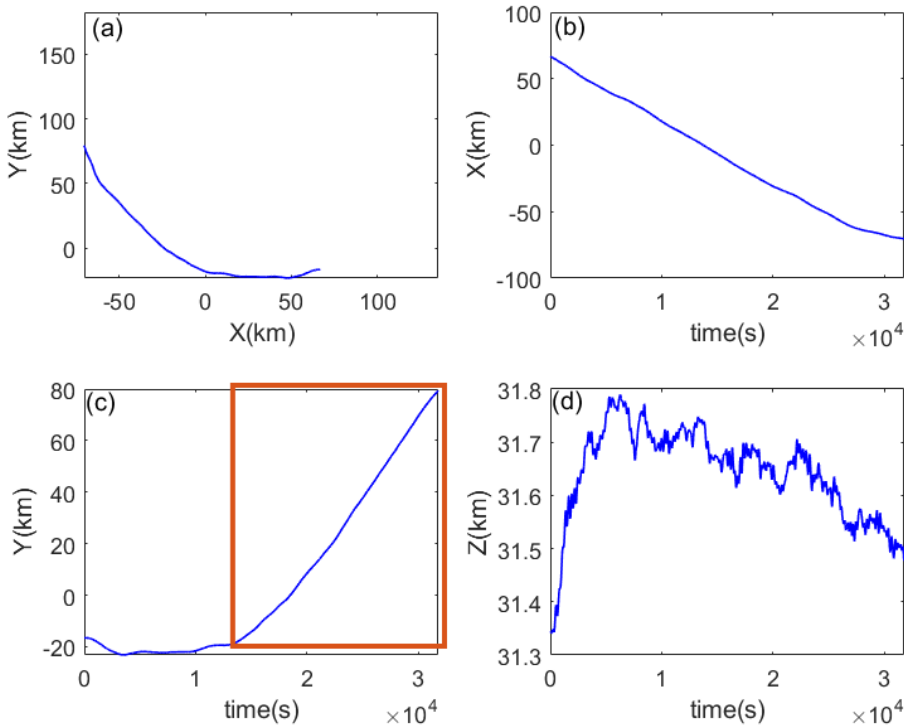


Figure R1. (a) The trajectory in the XOY plane, and the (b) X coordinate, (c) Y coordinate, and (d) Z coordinate during flat-floating stage.

In order to ensure straight line fitting, it is necessary to screen the flat drift trajectory and select the region that can be approximated as a straight line for linear fitting (as suggested by the reviewer). The selected period is represented by the red rectangular box in Figure R1. Then the data part that can be processed by line fitting is obtained in Figure R2.

At this time, the flat floating balloon is moving approximately in a quasi-straight line in the northwest direction. Therefore, it is necessary to transform the original zonal and meridional wind components into the directions parallel (u_L) and perpendicular (u_T) to the separation distance through coordinate transformation, as shown in Figure R8.

At this point, the original XOY coordinate system is rotated parallel to the linear fitting direction, and the separation distance and wind velocity components u_L and u_T are calculated in the new coordinate system.

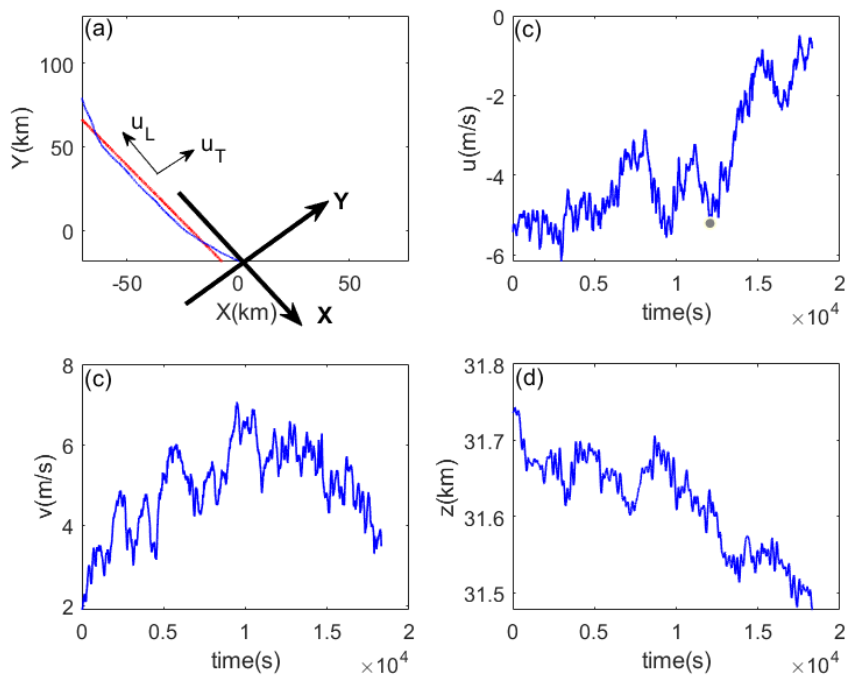


Figure R2. (a) The trajectory in the XOY plane, and the (b) X coordinate, (c) Y coordinate, and (d) Z coordinate for line fitting section.

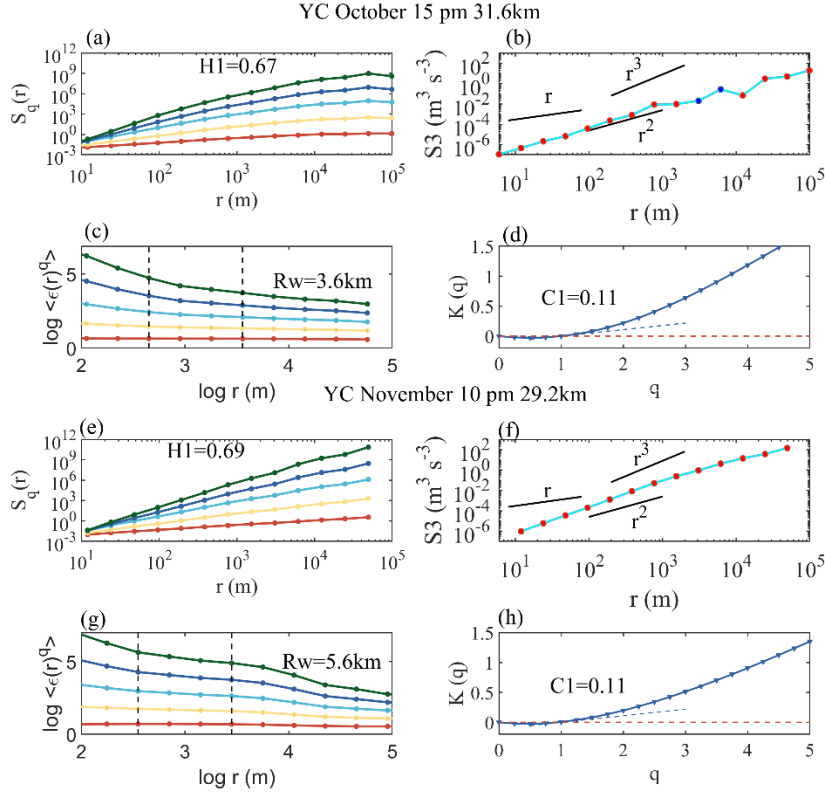


Figure R3. (a) Multi-order structure function, (b) third-order structure function, (c) multi-order singular measure and (d) slope $K(q)$ obtained from Yichang site at October 15 pm, and (e) multi-order structure function, (f) third-order structure function, (g) multi-order singular measure and (h) slope $K(q)$ obtained from Yichang site at November 10 pm.

Then, we calculated the disturbance parameter results under the new method, as shown in Figure R3, the figure also contains Yichang case at November 10 pm. Clearly we found some differences between the post-fitting and pre-fitting results.

Take Yichang case at November 10 pm as an example to illustrate the difference between the results before and after fitting. The result is shown in Figure R10.

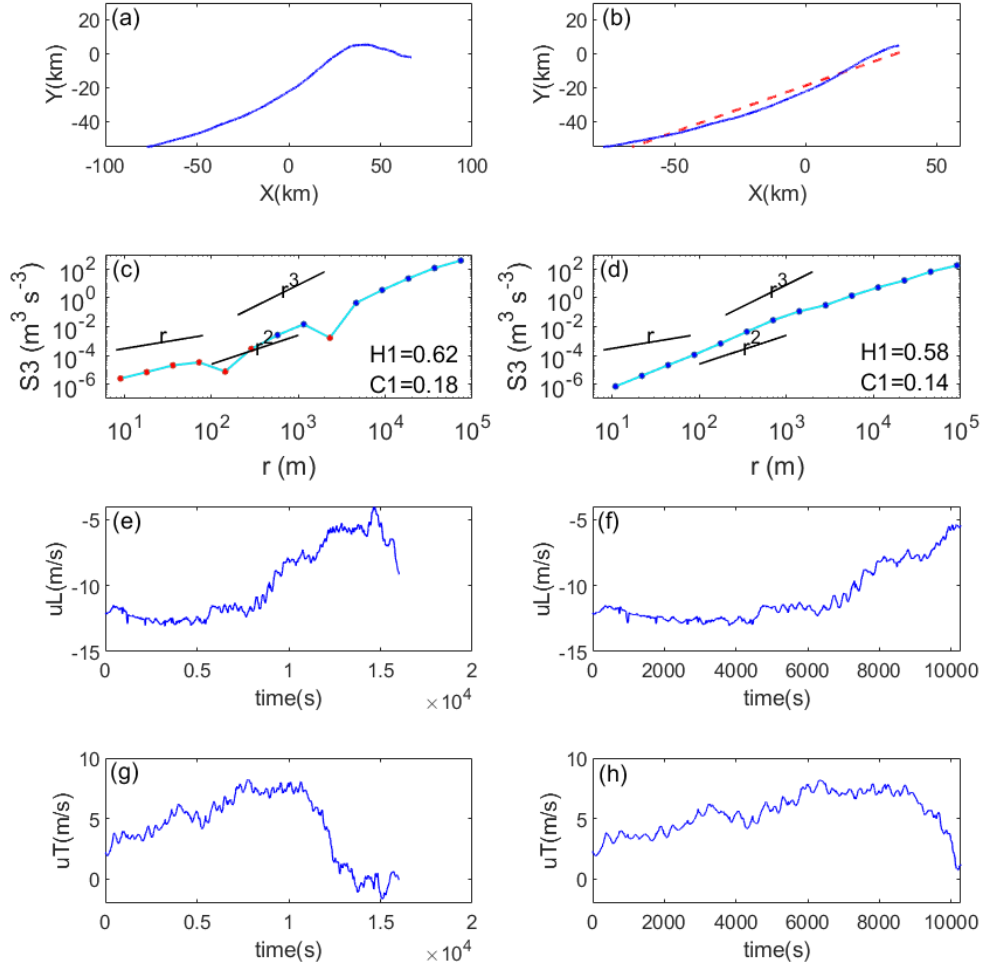


Figure R4. (a) The trajectory in the XOY plane before fitting, (b) The trajectory in the XOY plane within the fitting segment, (c) third-order structure function before fitting, (d) third-order structure function within the fitting segment, (e) the longitudinal (along the path) velocity before fitting, (f) the longitudinal (along the path) velocity within the fitting segment, (g) the transverse (normal to the path) velocity before fitting and (h) the transverse (normal to the path) velocity within the fitting segment obtained from Yichang site at November 10 pm.

It can be clearly seen from Figure R4 that the third-order structure functions of the two are significantly different before (left panel) and after (right panel) fitting. The reason for this is that in the process of linear fitting, in order to ensure the approximate straight line of the trajectory, partial curves and trajectories that deviate significantly from the straight line are omitted (this treatment is used in all data sets). According to equation 1 in the manuscript, the inconsistency between the convergence and divergence of velocity on adjacent scales leads to internal instability. The balloon itself moves with the wind, so when there is a sudden change in the velocity field, the trajectory of the flat drift will naturally change. For example, in Figure R10a, the balloon shifts from moving north to moving south near $X=40\text{km}$, which is caused by changes in wind field fluctuations, and can reflect the instability of atmospheric disturbance. When linear fitting is carried out, in order to ensure that the longitudinal velocity is basically along the moving direction, this part of the trajectory needs to be omitted, as shown in Figure R4b. In addition, after this treatment (linear fitting), the omitted part also corresponds to the large fluctuation region of the wind

field (Figure R4e-h).

In Lu's study (2008), they also pointed out that the two scales (for example, inconsistency in the direction of the energy cascade in Figure R4c) are related to different physical flow regimes. In balloon observations, this different physical flow regimes will be represented by curved (non-linear) trajectories. Therefore, in order to retain this recognition of different physical flow regions, we chose zonal or meridional projection (which can decompose the curved trajectory into zonal or meridional).

However, with your encouragement and suggestion, we decided to supplement the information in the straight line part. Here we compare the statistical results of the two processing methods. These two data sets can also reflect two scenarios: the scenario that includes the direction change of wind component (before fitting, zonal or meridional projection was adopted) and the scenario that does not include the direction change of wind component (within the fitting segment, the separation distance follows the direction of the fitted line). In simple terms, it is divided into the case that covers all physical flow regimes (before linear fitting) and the case that only considers a single physical flow regime (after linear fitting).

Since more flat drifting trajectories are very irregular, if you select a part that is approximately straight, you can only get a significantly smaller data segment, and many structure functions at a larger separation distance cannot be calculated. At the same time, even if the part that approximates a straight line is selected, there are actually many small fluctuations superimposed on it, which cannot be completely regarded as a straight line. At this time, interpolation at equal distances will cause errors. So our point of view is that no matter what kind of processing method, the error is unavoidable, and according to the characteristics of the flat float segment data, the decomposition of the latitude and longitude can make full use of the data.

As for processing on a time basis, I hope you could understand that we have not supplemented this practice here. One reason is that the amount of work in a manuscript is sufficient considering that, after supplementing the results of linear fitting, it is already possible to cover both the results containing different physical flow regions and the results containing only a single physical flow. Another reason is that small scale gravity waves on the spatial scale cannot be investigated with time interpolation. Of course, your suggestion is very good, and we will try it in the follow-up work.

3) L95-L97: The flight segments used for analysis should be chosen carefully in order to be quasi horizontal. For example, in part of the profile in Figure A1, after the burst of the outer balloon, the platform adjusts to its equilibrium level a few hundred meters below the burst altitude. In my understanding, the authors are nevertheless using that initial segment in their analysis, even though it is contaminated by altitude variations. I would recommend to discard it.

Response: We are very sorry that our presentation may have caused you to have such a misunderstanding. In fact, when selecting the data of the flat drift section, we have already omitted the period just after the end of the rising stage.

We strictly select each detection by manual screening, in order to select the segment with ideal flat-floating effect for subsequent calculation. In other word, we have already

discarded the initial segment after the burst of the outer balloon.

Thanks for your comments, to make the expression clearer, we make the following modifications:

L97 Added “It should be noted that, after the burst of the outer balloon, the platform adjusts to its equilibrium level a few hundred meters below the burst altitude (Figure A1), thus the initial segment after the burst of the outer balloon is also discarded.”

4) L115-120: Using structural functions, the calculation of the longitudinal velocity (Parallel to separation distance), requires careful consideration. Why not directly use the original flat drift data? what is the purpose of decomposition? Specifically, what criteria is used for reference to decompose according to the longitude direction or the latitude direction? Can the data analysis performed after the decomposition still represent the characteristics of the fluctuation?

Response:

Why not directly use the original flat drift data? what is the purpose of decomposition?

Because the original flat drift trajectory is not regular, if the separation distance direction is determined by linear fitting according to the original flat drift trajectory, part of the important flat-floating segment (that is, the area with significant wind field fluctuations) will be omitted. In order to illustrate this problem, we choose an example to explain:

Let's take WH case at October 18 pm as an example to illustrate it. In this example, the calculated $K(1)$ is 0.04.

The result of the flat-floating trajectory is shown in Figure R5. This is projected in the meridional direction. It should be noted that the two red rectangles in Figure R5a are dominated by the zonal displacement. In Figure R5c, the periods with small Y displacement over time are the periods between 0-593s and 9111-11500s, respectively.

We also plot the change of zonal and meridional winds over time, as shown in Figure R6. In this case, the longitudinal velocity (u_L) is the meridional wind component (v). According to the formula 5-9, the larger value of $K(1)$ is mainly due to the larger ensemble average value of the velocity increment (that is, the ensemble average of the longitudinal velocity difference over the separation distance r on the whole data).

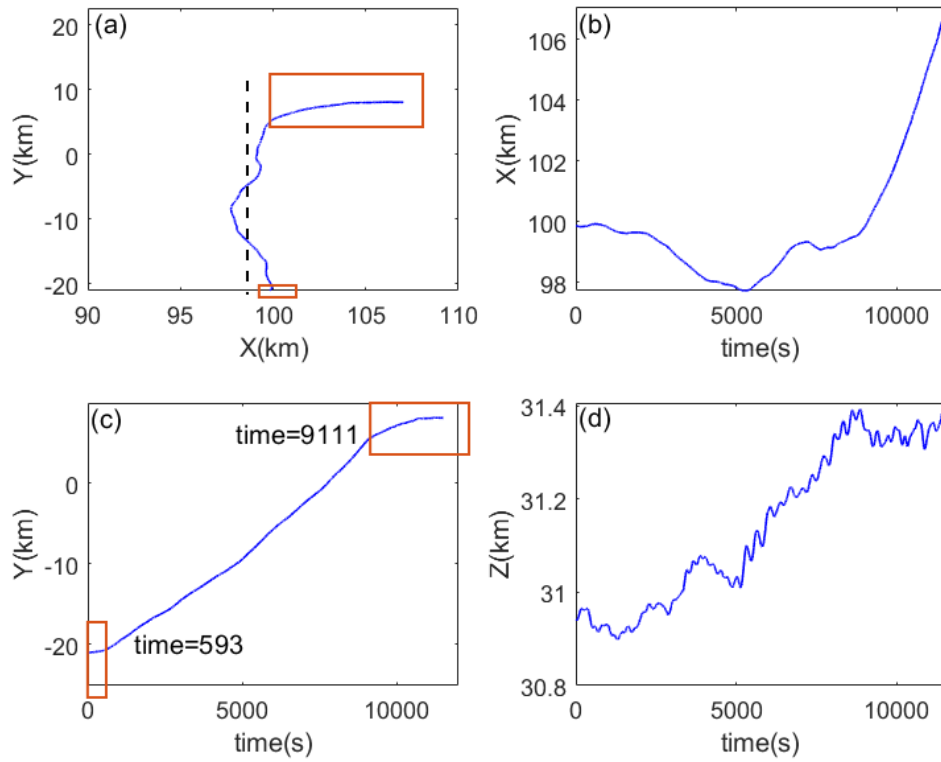


Figure R5. (a) The trajectory in the XOY plane, and the (b) X coordinate, (c) Y coordinate, and (d) Z coordinate during flat-floating stage.

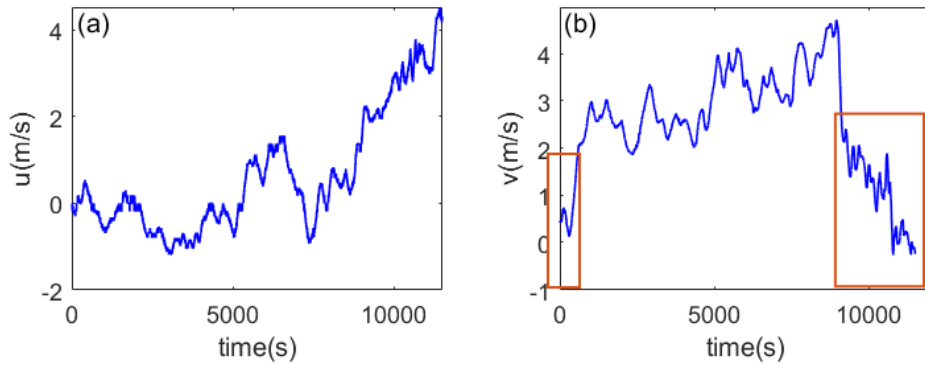


Figure R6. (a) zonal wind component, and (b) meridional wind component

In Figure R6, the longitudinal velocity increment in the two red rectangular boxes (the same time period as in Figure R5) has several segments for the sudden increase velocity, and the presence of these segments causes the $\delta u_L(r)$ value to be larger.

Due to the trajectory characteristics of this detection, it is not suitable for linear fitting (not satisfied with the premise of monotonically increasing or decreasing). However, if we discard the data segment in the red rectangular boxes and calculate along the zonal direction (this is also the way to use linear fitting for this case, and the fitting direction is the black dashed line in figure R5a), we can recalculate the $K(1)$ value to 0.004. This shows that some of the original detection trajectories are too irregular in the process of zonal or

meridional projection and can not satisfy the decomposition of this direction.

However, we have added to the revised version of the manuscript the results of the calculation after fitting a straight line along the trajectory (leaving out the irregular curved trajectory). Both these and the results of the zonal/meridional decomposition are presented in the manuscript. One reason is for comparison of the results containing different physical flow regions and the results containing only a single physical flow region, and the other reason is to explore whether the presence of strong wind field fluctuations (before and after linear fitting) will affect the correlation between the calculated small-scale gravity wave parameters and other disturbance parameters.

Specifically, what criteria is used for reference to decompose according to the longitude direction or the latitude direction?

We take the direction of the longer projection distance as the separation distance direction.

Specifically, if the line from the start point to the end point of the flat-floating segment is longer in the projection along the zonal (meridional) direction, the zonal (meridional) direction is chosen as the separation distance direction.

Can the data analysis performed after the decomposition still represent the characteristics of the fluctuation?

Since the wind field always comes from a combination of two directions (meridional and zonal), our selection of one direction as the separation distance direction actually reflects only part of the characteristics of the wave. Of course, the best way is to adopt the method of linear fitting, but the data segment of linear fitting is limited, and the overly curved trajectory cannot be covered, and this part of the content contains important fluctuation information.

Therefore, in order to take into account the region of strong fluctuations and the fluctuation information of the synthesized wind direction, we give the results of taking the latitude/longitude direction as the separation distance direction and the fitting straight line as the separation distance direction in the manuscript.

5) L154-L161: Why was the gravity wave scale chosen to be 5km? Considering the different horizontal resolutions of different data, the specific scale of gravity waves selected should be different. Therefore, I understand that the author here should choose the wave parameter closest to 5km, and suggest that the author give the statistical distribution results of the actual scale.

In addition, considering that the flat-floating distance is long enough, why not choose a longer scale, and whether this will cause a difference in the analysis results?

Response: Sorry for this gross oversight, but the threshold set in our program is 6km.

The scale of gravity waves comes from a separation distance r less than 6 km and closest to 6km. The statistical characteristics of H1 and C1 at the corresponding scale were used as the quantization of perturbation parameters of small-scale gravity waves at this scale, which was applied in earlier studies.

we make the following modifications:

L159 Changed “and the separation distance closest to 5 km (< 5 km)”

To “and the separation distance closest to 6 km (< 6 km)”.

In fact, choosing the scale closest to 6km can not only satisfy the statistical quantity of

parameter results, but also ensure the robust of velocity increment on this scale. We now take the data from Wuhan on October 23 as an example to explain this choice.

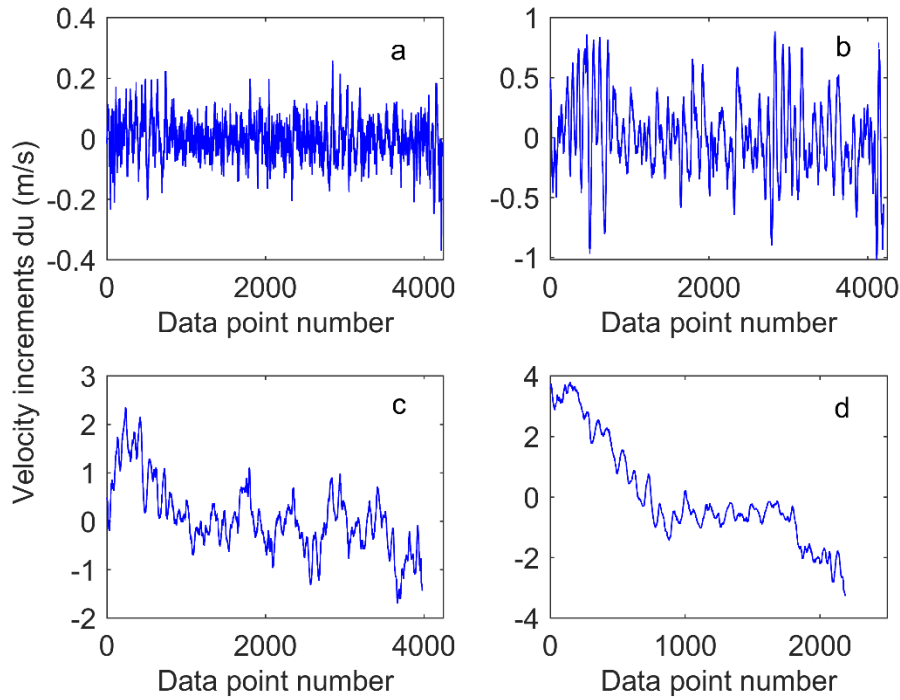


Figure R7. Velocity increments calculated from beginning to end in the data series where the separation distances are (a) 64 m, (b) 512 m, (c) 4096 m, and (d) 32 768 m, respectively.

Since the structure function is a statistical feature and we only focus on small-scale GWs (within a few kilometers) and turbulence, the deviation of the structure function which may be caused by the obvious change of the floating height on a larger scale (the influence of floating height on the statistical characteristics of velocity increment gradually increases, as shown in Fig. R7) is not within the scope of our discussion. Therefore, the results are reasonable and reliable.

With the increase of the selected scale, the set of data points of the speed increment du decreases, and its fluctuation value becomes more and more distinguishable. That is, too long a scale will cause significant differences in the velocity increments du , and the result will be no longer robust and cannot be used to calculate $H1$ and $C1$.

At the same time, we supplement the statistical results of the selected gravity wave scale, shown in figure R8.

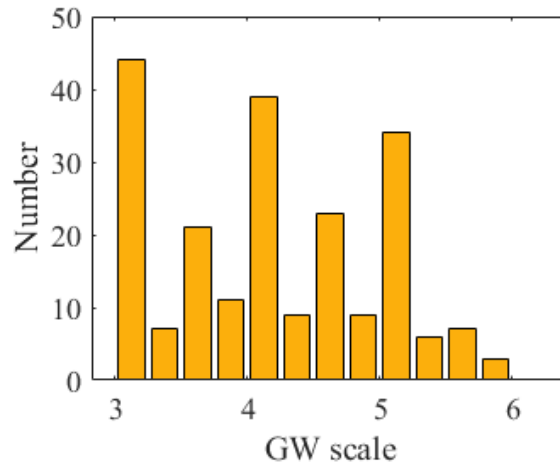


Figure R8. Histogram of gravity wave scale.

6) L167-L169: How does the author determine this conclusion? It is suggested that the author add relevant explanations (figures or tables) in this work.

Response: Thanks for your comments, we make the following modifications:

Changed “The velocity increments $\delta u_L(r)$ is the key process for calculating the disturbance parameters from flat-floating data, and has shown good robustness within the separation distance of small-scale gravity waves and turbulence (He et al., 2022a). thereforeTherefore, the results will not be affected by the fluctuation of flat-floating height, as well as the swing of the balloon.”

to “The velocity increments $\delta u_L(r)$ is the key process for calculating the disturbance parameters from flat-floating data, and has shown good robustness within the separation distance of small-scale gravity waves (Figure A2). In fact, choosing the scale closet to 6 km (less than 6 km) can not only satisfy the statistical quantity of parameter results, but also ensure the robust of velocity increments on this scale. With the increase of the separation distance, the fluctuation of velocity increments becomes more and more distinguishable. That is, too long a scale will cause significant differences in the velocity increments δu at different data points, and the result will be no longer robust and cannot be used to calculate H1 and C1. Therefore, the selected SGW scale of 6 km will not be affected by the fluctuation of flat-floating height, as well as the swing of the balloon.”

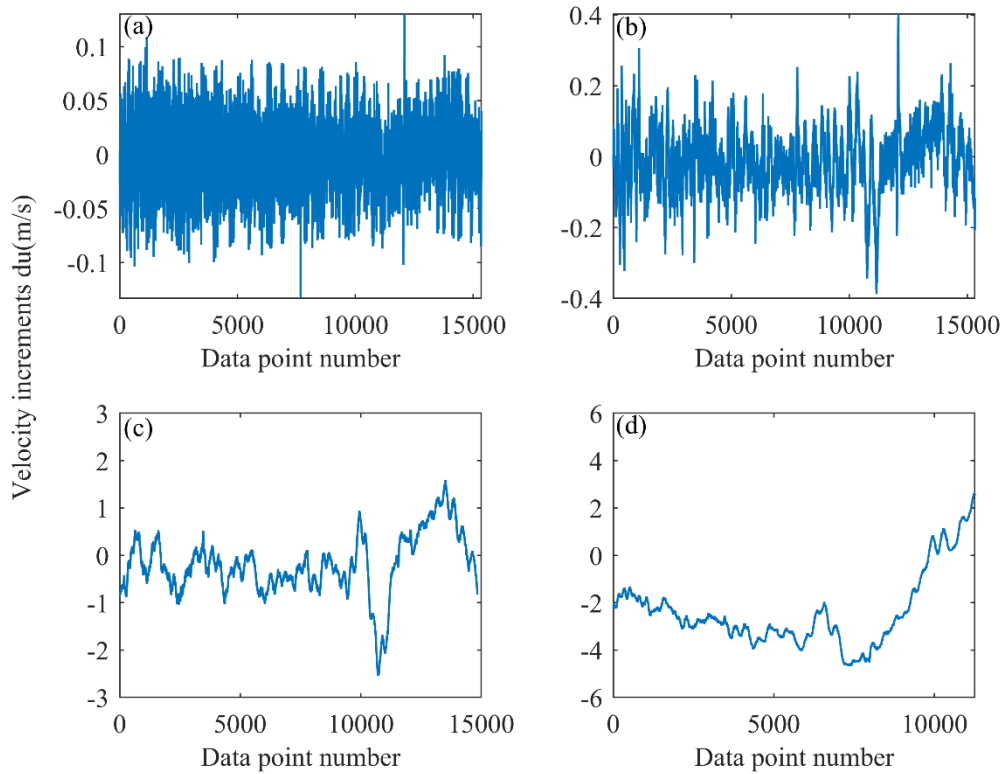


Figure R9. Velocity increments calculated from beginning to end in the data series from Yichang site on November 8, where the separation distances are (a) 44 m, (b) 352 m, (c) 5600 m, and (d) 45 056 m, respectively.

7) From Figure 2, according to my understanding, the Hurst parameter $H1$ and intermittency parameter $C1$ both come from the calculation of the slope. If so, the slope of $H1$ is easily understood, which comes from the linear fitting of the structure function spectrum in Figure 2a. However, how is the slope of $C1$ calculated in Figure 2d?

Also, how to determine the premise of Eq. (9)? Given a nonstationary random atmospheric process with stationary increments that is scale invariant from some outer scale R down to some inner scale η , I wonder whether the relationship $K(1)=0$ can always be satisfied when calculating the intermittent parameter $C1$? In other words, how is approximately close to 0 (L166) defined, and does it eliminate part of the result?.

Response: In response to the first question, we make the following modifications:

L175 Changed “Figure 2c is the relationship between the q -order singularity measure $\langle \varepsilon(r; x)^q \rangle$ and the separation distance r in log-log coordinate, through which $C1$ is calculated with a value of 0.08 (Figure 2d).”

To “Figure 2c is the relationship between the q -order singularity measure $\langle \varepsilon(r; x)^q \rangle$ and the separation distance r in log-log coordinate. The curves $q=1, q=2, q=3, q=4,$ and $q=5$ are given, from which the slope values can be calculated within the selected SGW scale (left of the black dashed line) as $-K(1), -K(2), -K(3), -K(4),$ and $-K(5)$, respectively. Then the variation curve of $K(q)$ with q can be obtained in Figure 2d, where $q=0, 0.25, 0.5, \dots, 5$. The fitting slope of the $K(q)$ curve at $q=1$ is calculated from the $K(q)$ values

corresponding to $q=0.75$, $q=1$, and $q=1.25$, and this slope value is defined as intermittent parameter $C1$.”

In response to the second question, allow me to explain the problem from two aspects :

a. Based on mathematical formula.

Based on the mathematical formula 9, to obtain the value of $C1$, the numerator and denominator must both approach 0 as q approaches 1, thus obtaining the value of $C1$ according to the L'Hôpital's rule. The derivation of $C1$ is given in detail in Marshak et al, 1997.

b. Analysis based on specific cases.

Let's take WH case at October 18 pm as an example to illustrate it. In this example, the calculated $K(1)$ is 0.04.

The result of the flat-floating trajectory is shown in Figure R5. This is projected in the meridional direction. It should be noted that the two red rectangles in Figure R5a are dominated by the zonal displacement. In Figure R5c, the periods with small Y displacement over time are the periods between 0-593s and 9111-11500s, respectively.

We also plot the change of zonal and meridional winds over time, as shown in Figure R6. In this case, the longitudinal velocity (u_L) is the meridional wind component (v). According to the formula 5-9, the larger value of $K(1)$ is mainly due to the larger ensemble average value of the velocity increment (that is, the ensemble average of the longitudinal velocity difference over the separation distance r on the whole data).

In Figure R6, the longitudinal velocity increment in the two red rectangular boxes (the same time period as in Figure R5) has several segments for the sudden increase velocity, and the presence of these segments causes the $\delta u_L(r)$ value to be larger.

Due to the trajectory characteristics of this detection, it is not suitable for zonal decomposition (not satisfied with the premise of monotonically increasing or decreasing along the zonal). However, if we discard the data segment in the red rectangular boxes and calculate along the zonal direction (this is also the way to use line fitting for this case, and the fitting direction is the black dashed line in figure R5a), we can recalculate the $K(1)$ value to 0.004. This shows that some of the original detection trajectories are too irregular in the process of zonal or meridional projection and can not satisfy the decomposition of this direction.

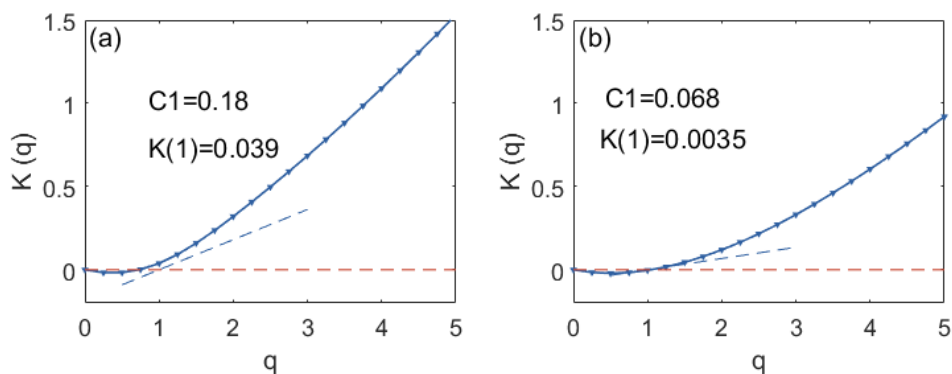


Figure R10. slope $K(q)$ obtained (a) before and (b) after linear fitting.

When considering all physical flow regions (as mentioned in our previous reply), $K(1)$

serves as a threshold to exclude the conditions that do not satisfy the statistical characteristics of the intermittent parameters in this case. Our definition of $K(1)$ approximately close to 0 in this manuscript means that $K(1) < 0.01$.

When $K(1)$ exceeds this value, we consider that the data series does not satisfy an unstable process with stable increments. It can also be intuitively seen from the $K(q)$ curve that $K(1)$ and 0 have a certain distance. This means that the trajectory is too curved and irregular, or the actual detection of wind speed has too much wild value (from the positioning system of excessive error).

we make the following modifications:

L166 Added “Here $K(1)$ approximately close to 0 is defined as $K(1) < 0.01$. When $K(1)$ exceeds this value, it can be intuitively seen from the $K(q)$ curve that $K(1)$ and 0 have a certain distance. The physical explanation behind it is that the flat-floating trajectory is too irregular, or the actual detected wind speed has too many wild values (abnormalities from the positioning data).”

8) L173-L175: “From third-order structure function, a downscale energy cascade (from large to small scales) can be seen from the third-order structure function”.

How do you know this conclusion? Do red dots (negative values) represent downscale energy cascade, corresponding to a drag of gravity wave on background, while blue dots (positive values) denote upscale energy cascade corresponding to an increase in turbulent kinetic energy? I think the authors should use more approachable language that explains its physical meaning.

Response: Yes, red dots (negative values) represent downscale energy cascade, corresponding to a drag of gravity wave on background, while blue dots (positive values) denote upscale energy cascade corresponding to an increase in turbulent kinetic energy.

Based on Kolmogorov theory, Lindborg (Lindborg, 1999) obtained the ideal theoretical relationship for two-dimensional turbulence by reprocessing. Experiments show that the third-order structure function is superior to the second-order structure function in analyzing turbulence (Cho & Lindborg, 2001; Lindborg & Cho, 2001). The third-order structure function can not only eliminate the arbitrariness of the universal constant in the power law expressed by the second-order structure function in physical space, but also reflect the direction of the energy cascade through the sign of the value, where negative values represent downscale energy cascades and positive values represent inverse scale energy cascades. And this conclusion is obtained from above researches.

The direction of the energy cascade can be obtained from equation 1. Since E is the energy dissipation rate, when $S_3(r)$ is positive, E is negative, meaning that energy is transferred from small to large scales. when $S_3(r)$ is negative, E is positive, meaning that energy is transferred from large to small scales.

Thanks for your comments, we make the following modifications:

L121 Changed “A positive value of $S_3(r)$ represents upscale energy cascades (from small to large scales), while a negative value of $S_3(r)$ represents downscale energy cascades (from large to small scales) (Lindborg, 1999).”

To “The relationship between the third-order structure function and the energy transfer can be obtained by Eq. (1). When $S_3(r)$ is positive, E is negative, energy transfers from small to

large scales, meaning upscale energy cascades. When $S_3(r)$ is negative, E is positive, energy transfers from large to small scales, meaning downscale energy cascades.”

9) L180: The curve in Figure 2d increases as q increases. Could you make more explanations on the physical meaning of $K(q)$? What does the larger or smaller $K(q)$ (i.e., intermittent parameter) mean?

Response: In fact, $K(q)$ is not an intermittent parameter, $K(q)$ is the fitting slope of $\langle \varepsilon(r)^q \rangle$ and r in the log-log coordinate system, where q is the order. The intermittent parameter is the slope of the tangent of the curve of $K(q)$ at $q=1$. The intermittency parameter is defined to measure the singularity of a fluctuation. The more singular a fluctuation, the larger the intermittency and the fewer the information dimensions, resulting in the fluctuation being more like the Dirac delta function. With this interpretation, the intermittency can be understood as an information codimension of the fractality of a process.

The value of the intermittency parameter is typically in the range of $0 \leq C1=K'(1) \leq 1$.

The larger $C1$ is, the more obvious the characteristic of turbulent activity is. In general, 0.2-0.3 can already represent significant turbulence. In the current investigation results, the value of $C1$ in the turbulence occurrence data is also in this range. (plasma physics study by Carreras et al. (2000) came up with values for intermittency in plasma turbulence ranging from 0.15 to 0.30,

10) I90-192: This statistical result is very interesting, and it is recommended that the author supplement its physical explanation.

Response: In our previous discussion, it has been shown that when the flat-floating trajectory is significantly curved (the trajectory is not straight), it indicates that there are different physical flow regions in the detection region, and when this part of the curved trajectory is not omitted, bidirectional energy cascades can often be found in the obtained third-order structure function, which means the instability of the wind field fluctuation.

When the value of $H1$ is smaller, the instability of the data series is stronger. In the trajectory diagram drawn, the flat-floating trajectories of the six sites in autumn are more irregular, indicating more frequent different physical flow regions, and internal instability is more likely to occur.

Thanks for your comments, we make the following modifications:

L192 Added “It is reasonable to have a lower $H1$ distribution in autumn, since the flat-floating trajectories of the six sites in autumn are more irregular. The obvious change in the trajectory (away from the previous straight direction) indicates that the detected data contains different physical flow regions, suggesting internal instability of the background wind field fluctuations and some multifractal characterizations.”

11) Explanation of the jagged structure in the spectral shape.

By comparing the results of Figure 2 and Figure 3, we can see some differences in the results:

a) Compare (a) in Figure 2 with (a) and (e) in Figure 3, multi-order structure function has

obvious spectral shape difference on large scale (larger than 10km). What is the difference behind this difference in the actual observed wind field? It is suggested that the authors add relevant explanations.

b) Compare (b) in Figure 2 with (b) and (f) in Figure 3, third-order structure function has obvious the sawtooth structure in the spectral shape in Figure 3 (b) and (f), while the spectral shape in Figure 2 (b) is much smoother. Can sawtooth be considered a special spectral structure that appears when atmospheric disturbances are strong?

Response: To illustrate the first problem, we plot the longitudinal velocity component and flat-floating trajectory of the three cases (stable gravity wave, unstable gravity wave, and the coexistence of gravity wave and turbulence) as shown in Figure R11. The obvious spectral shape difference on large scale (larger than 10 km) mainly comes from the intervals with significant inclinations accompanied by a relatively large increase or decrease in the speed increment $u_L(r)$ on these intervals. Since $S_q(r) = \langle |\delta u_L(r)|^q \rangle$, when the curve of multi-order structure function at a certain separation distance r has an obvious inflection point, it means that there is a sudden increase or decrease of some velocity increment in the set of all velocity increment at this scale.

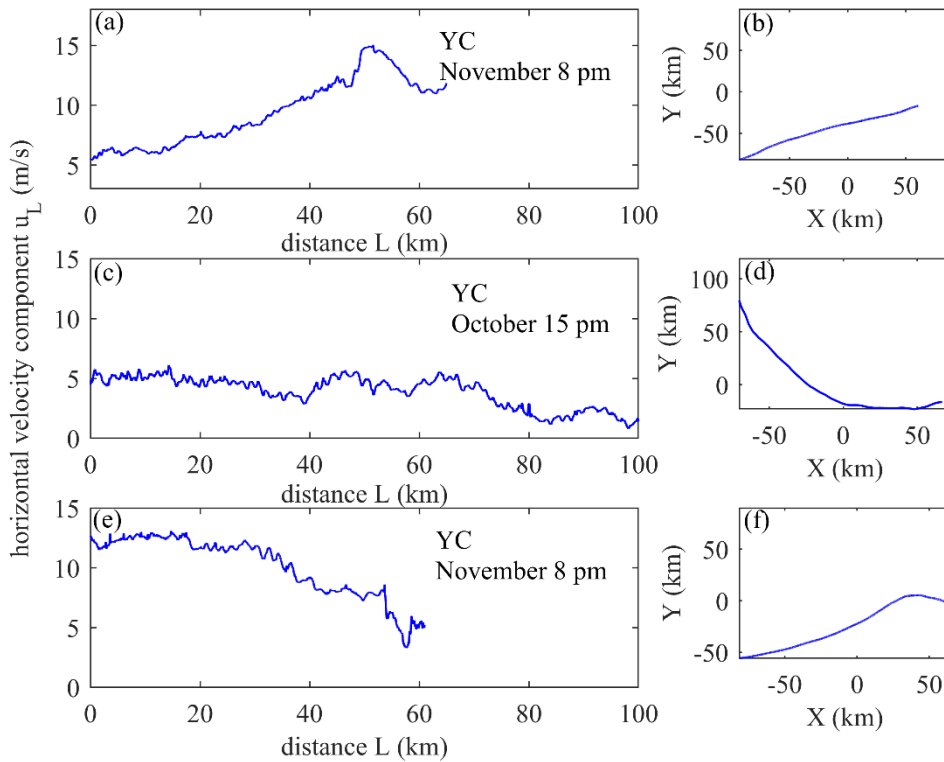


Figure R11. The variation of horizontal velocity component u_L along the zonal separation distance (left panel) and flat-floating trajectory (right panel) from three cases.

To illustrate the second problem, we observe the trajectories of three cases. For the stable gravity wave (Yichang site on November 8), the flat-floating trajectory moves approximately along a quasi-straight line, reflecting a relatively single physical flow region, which indicates that the internal instability of atmospheric wind field fluctuations is relatively weak. For the unstable gravity wave (Yichang site at October 15 pm) and the coexistence of gravity waves and turbulence (Yichang site at November 10 pm), the flat-

floating trajectory has been significantly deflected, indicating that the detection area contains different physical flow regions, which means that the internal instability of atmospheric wind field fluctuations is relatively strong. Obviously, this also caused the sawtooth structure in the spectral shape and the inconsistency in the energy cascade direction of the third-order structure function.

Thanks for your comments, we make the following modifications:

L187 Added “By comparing the case results of Figure 2 and Figure 3, multi-order structure function (third-order structure function) can be found to have the spectral shape differences on certain scales, which mainly comes from the intervals with significant inclinations accompanied by a relatively large increase or decrease in the speed increment $u_L(r)$ on these intervals (Figure A3). Since $S_q(r) = \langle |\delta u_L(r)|^q \rangle$, when the curve of $S_q(r)$ at a certain separation distance r has an obvious inflection point, it means that there is a sudden increase or decrease of some velocity increment in the set of all velocity increment at this scale (He et al., 2022a).

For the stable gravity wave (Yichang site on November 8), the flat-floating trajectory moves approximately along a quasi-straight line (Figure A3b), reflecting a relatively single physical flow region, which indicates that the internal instability of atmospheric wind field fluctuations is relatively weak. For the unstable gravity wave (Yichang site at October 15 pm) and the coexistence of gravity waves and turbulence (Yichang site at November 10 pm), the flat-floating trajectory has been significantly deflected (Figure A3d and A3f), indicating that the detection area contains different physical flow regions, which means that the internal instability of atmospheric wind field fluctuations is relatively strong. Obviously, this also caused the sawtooth structure in the spectral shape and the inconsistency in the energy cascade direction of the third-order structure function.

”

12) L199-L206: I think the author's method here for calculating inertial gravity waves and turbulence is too simplistic. The author is strongly advised to further elaborate on the details. Taking into account the specific nature of the journal, detailed and complete discussion is encouraged.

For example, what is the calculated altitude interval of the turbulence parameter? Are the statistical results from the regional average or the regional sum?

In addition, considering that there are already many observations of inertial gravity waves and turbulence, it is recommended to increase the comparison between the relevant parameters of this article and the existing results to further illustrate the rationality and reliability of the results.

Response: Thanks for your comments, we fully agree with your suggestion and make the following modifications:

a) The expression of method introduction is expanded and the introduction to methods is moved to section 3.

Added “Since turbulence is highly intermittent, the turbulence parameters obtained here are derived from the regional average of non-zero values (turbulence exists) within the height range of 15-25 km of each profile.”

b) The comparison with the IGW and turbulence parameter results of other studies is

supplemented.

L217 Added “In this paper, the vertical wavelength of the IGW is concentrated in the range of 1~3 km, which is close to the scale of the stratospheric IGW in China (1.5~3 km) observed by radiosonde data (Bai et al., 2016). In our results, kinetic energy and potential energy of IGW are concentrated at 2~6 J/kg and 0~2 J/kg, respectively. In the tropics, by contrast, the kinetic energy of stratospheric IGW has already exceeded 10 J/kg (Nath et al., 2009), indicating more intense wave activity at lower latitudes. The turbulent kinetic energy dissipation rate $\log_{10}\epsilon$ is between -5 and -2 from RTISS, which is comparable to those obtained based on radiosonde data in the United States from -4 to $-0.5 m^2s^{-3}$ (Ko and Chun, 2022) and in Guam from -6 to $0 m^2s^{-3}$ (He et al., 2020a).”

13) L255: In Figure 7, the authors illustrate the correlation between the different parameters by drawing a scatter plot. However, due to the limited sample size, some linear relationships are not obvious, which makes some of the author's statements seem a little absolute. For example, L267-L270: The trend of increasing first and then decreasing is not obvious, so it is suggested that the author delete this expression.

Also, If the author tends to discuss the relationship between inertial gravity waves and small-scale gravity waves, the relatively absolute wording is modified to a mild expression. Because in the present work of the authors (if the number of current observations cannot be significantly increased), due to the limitations of the sample, it is also necessary to discuss the possibility that the maximum or minimum value of the edge region in the scatter results is caused by the wild value.

Response: Thanks for your comments, we fully agree with your suggestion and make the following modifications:

a) Deleted the place where the expression of relevance is not obvious.

Deleted “The turbulent kinetic energy dissipation rate (ϵ) increases first and then decreases with the increase of KHI (Figure 7h). This is because the increase of KHI is conducive to the generation of turbulence, however, when the KHI reaches a certain threshold value, the turbulent layer cannot be maintained and begins to decay, resulting in a weakening of turbulence activity (He et al., 2020b).”

b) To discuss the possibility that the maximum or minimum value of the edge region in the scatter results is caused by the wild value.

We recalculated H1 and C1, where quality control and pre-judgment were performed for each selected flat-floating segment. Considering that the calculation of wind speed comes from the coordinates of the positioning system, the pre-judgment is to observe the difference between longitude and latitude at adjacent times. If the curve has no outlier value, it indicates that the positioning system works normally in the flat drift stage, and the obtained wind speed is also credible.

The judgment method is shown in Figure R12, left panel shows the case where the positioning data is abnormal, and right panel shows the case where the positioning data is normal.

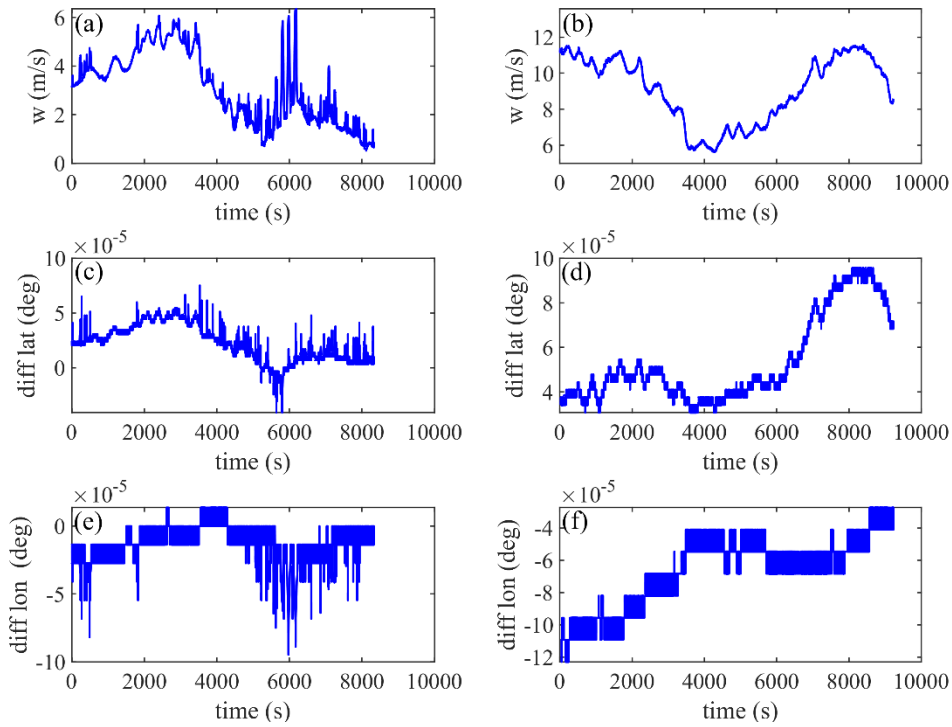


Figure R12. (a) wind velocity, (c) latitude difference, and (e) longitude difference for the case where the positioning data is abnormal, and (b) wind velocity, (d) latitude difference, and (f) longitude difference for the case where the positioning data is normal

Obviously, the difference of positioning coordinates in adjacent time can identify the abnormal situation of positioning data, that is, there are a large number of wild values in a stable increment. Even if there is a sudden increase in wind speed, the transformation of the positioning data should be continuous, and this wild value comes from the anomaly of the signal received by the positioning system. So the data in this case is discarded.

Under this premise, the presence of larger C1 values can completely eliminate the interference of outlier values. Although the sample size of a large C1 value (>0.15) is relatively small (because strong detection of intermittent parameters is inherently a small probability event in the total sample), it is still possible to see that a large C1 does correspond to a weakened inertial gravity wave below.

According to your suggestion, we make the following modifications:

L195 Added “Considering that the calculation of wind speed comes from the coordinates of the positioning system, it is necessary to make sure that there is no wild value interfering with the results. The difference of positioning coordinates in adjacent time can identify the abnormal situation of positioning data, that is, whether there are obvious wild values in the difference of longitude or latitude. Figure A4 shows the cases for abnormal and normal positioning data, and these abnormal cases are screened out.”

L270 Added “Although the quantity of large C1 values (>0.15) is relatively rare (the detected disturbances with strong intermittence are still small probability events in the entire sample), it is still possible to see that the enhanced C1 is accompanied by the weakened IGW below.”

14) L282-L283: “Based on the ERA5 reanalysis data, the ozone mass mixing ratio (OMR) and PV at different pressure layers that matched the detection are selected”

How this is matched needs to be further explained.

Response: Thanks for your comments, we fully agree with your suggestion and make the following modifications:

Changed “Based on the ERA5 reanalysis data, the ozone mass mixing ratio (OMR) and PV at different pressure layers that matched the detection are selected. According to the latitude and longitude range covered by RTISS during flat-floating stage, the OMR and PV obtained from the ERA reanalysis data are averaged in the corresponding area”

To “Based on the ERA5 reanalysis data, the ozone mass mixing ratio (OMR) and PV at different pressure layers that matched the detection are selected. Specifically, the ERA5 data at 00UTC and 12UTC within the longitude and latitude range of the selected flat-floating stage are screened, and the value after regional average is used as the reanalysis data result corresponding to the flat-floating detection at that time.”

15) L354: What exactly do fingerprints mean here?

Response: What the author wants to express here is that the parameter space (H1 and C1) is used to related to changes in atmospheric composition indirectly. Considering that the expression may not be clear, we make the following modifications according to your suggestion:

Changed “Besides, the possible “fingerprint” of this parameter space in the material transport of other components (such as water vapor, carbon dioxide, methane, etc) in the stratosphere also deserves further attention.”

To “Besides, potential connections that may exist between this parameter space and other atmospheric components (such as water vapor, carbon dioxide, methane, etc) transported in the stratosphere also deserves further attention.”

Minor comments:

1) L65: The two colors in Figure 1 are not marked with seasons, please add.

Response: Thanks for your comments, according to your suggestion we have made the following modifications:

The figure has been redrawn to add a description of the colors.

2) L168: Where is Text S2?

Response: I am very sorry that this is an earlier version of the expression and it is not in the current manuscript. It has been deleted.

3) L200: 18–25km → 18–25 km.

Response: Thank you for pointing out this detail, and we have checked and corrected similar problems in the whole article.

4) L213: “critical layer filtering” should be further explained, for example, how are gravity waves affected here by the background wind field.

Response: Thanks for your comments, according to your suggestion we have made the

following modifications:

Changed “The dominant propagation directions of IGWs in summer and autumn are northeast and southwest respectively, due to the effect of “critical layer filtering” (Eckermann, 1995).”

To “The dominant propagation directions of IGWs in summer and autumn are northeast and southwest respectively, due to the effect of “critical layer filtering” (Eckermann, 1995). The background wind field filters out gravity waves propagating in the same direction, and passes through gravity waves propagating in the opposite direction.”

5) L220: The display in figure4 e and f is incomplete and the authors should readjust the boundary values.

Response: Thanks for your comments, according to your suggestion we have made the following modifications:

The figure is redrawn and the longitudinal scale ranges of the subgraphs e and f are adjusted.

6) L220: The two colors in Figure 1 are not marked with seasons, please add.

Response: Thanks for your comments, according to your suggestion we have made the following modifications:

The figure has been redrawn to add a description of the colors.

7) L235: The size of the ordinate scale in Figure 5b is inconsistent with other subgrams.

Response: Thanks for your comments, according to your suggestion we have made the following modifications:

The figure has been redrawn to adjust the smaller scale value in the vertical coordinate of the subgraph.

8) L253: between H1 → between H1

Response: Thanks for your comments, according to your suggestion we have made the following modifications:

Changed “between H1”

To “between H1”

9) L321-L324 100hPa → 100 hPa, 10hPa → 10 hPa

Please check for similar errors elsewhere.

Response: Thanks for your comments, according to your suggestion we have made the following modifications:

Changed “100hPa” to “100 hPa”

To “10hPa” to “10 hPa”

At the same time, we examined the entire manuscript and corrected for the occurrence of multiple spaces between words.

9) Unfortunately, neither my abilities nor my time allow me to find all the grammatical problems throughout the manuscript. Therefore, I sincerely ask the authors to check the full text by themselves, and preferably seek advice from a native speaker.

Response: Thank you for pointing this out. We have revised the whole manuscript once again, including the grammatical problems. I hope you could understand that there has been no specific language polishing given that the current version of the manuscript may still need to be revised. If you still feel that the language needs further improvement in the future, we will increase the language polishing in the subsequent revision.

At the end, Authors are grateful to the anonymous reviewer for providing valuable comments to improve the manuscript up to this level. We greatly appreciate the time and effort you put into improving the quality of my manuscript, and we have benefited immensely from your selfless comments and suggestions. Besides, if you have more suggestions or comments about my manuscript or the content of the reply, I will always be pleased to make timely replies and revisions and benefit from communicating with you. Finally, thank you again from the bottom of my heart.

In addition, the author also checked the full text, revised some grammar and details, and they can all be found with “track changes”.